

Effects of boundary conditions on confined optical phonons in semiconductor nanostructures

P. A. Knipp

Department of Physics and Computer Science, Christopher Newport University, Newport News, Virginia 23606-2998

T. L. Reinecke

Naval Research Laboratory, Washington, D.C. 20375-5347

(Received 15 June 1993)

The dependence of physically observable quantities such as electron-phonon scattering rates on the boundary conditions for the optical phonons confined in polar semiconductor quantum wells, quantum wires, and quantum dots are examined within the dielectric continuum approach. Calculations of the confined phonons and of their contributions to the scattering rates are made using the boundary conditions of Maxwell's equations at the interfaces and the condition that the ionic displacements go to zero there. These results are compared with the results obtained using only the condition that Maxwell's equations be satisfied (the usual dielectric continuum model). We find that in the absence of phonon dispersion the rates of scattering by the confined phonons in these two cases are *identical* even though the individual phonons differ. We attribute this result to the fact that physically observable quantities involve sums over complete sets of states. As a part of the present work we have derived an interesting relation between the contributions of the confined phonons and the interface phonons to the scattering rates in nanostructures. This relation is useful in, for example, obtaining the rates of scattering by the confined modes for geometries of low symmetry where straightforward sums are difficult.

I. INTRODUCTION

Optical phonons and the corresponding electron-phonon interactions in polar semiconductor nanostructures, including quantum wells, quantum wires, and quantum dots, have been the subject of intense study in recent years. A major focus of these studies has been on the effects of confinement on physical quantities such as the electron-phonon interactions and on the resulting scattering rates. Particular interest has been directed at the possibility that phonon confinement may affect significantly the scattering rates. The scattering of carriers by optical phonons controls carrier relaxation on the picosecond time scale and also determines room temperature mobilities, and thus it will be important in potential device applications of these structures. With recent developments in ultrafast spectroscopies these relaxation processes now are directly accessible experimentally, and they have attracted considerable attention recently.

Macroscopic approaches for the optical phonons of semiconductor nanostructures are especially attractive because they give analytic results for the electron-phonon interactions and make possible the treatment of scattering in systems with widely varying size and shape. The dielectric continuum approach¹ has proven to be particularly attractive. This approach yields "interface" phonons and "confined" phonons, both of which satisfy the "electromagnetic" boundary condition (BC) that the scalar potential be continuous across the interface. The interface phonons obtained from this approach agree well with those from lattice dynamics calculations.²⁻⁴ In addition, electron-phonon scattering rates calculated re-

cently for quantum well systems using microscopic lattice dynamics results for the phonons^{2,3} are in reasonably good agreement with those obtained from the dielectric continuum approach. However, lattice dynamics calculations²⁻⁴ demonstrate that, in addition to satisfying the electromagnetic BC, the ionic displacements \mathbf{u} of the confined phonons vanish at (or within an atomic layer of) the interface. In recent work^{2,3,5,6} it has been found that electron-phonon scattering rates have only a modest, but nonzero, dependence on the "mechanical" BC that \mathbf{u} goes to zero at the interface. At first this small effect on the scattering rates may seem surprising in that the confined phonons are modified substantially by this additional constraint.

In the present work we examine the dependence of physically observable quantities such as electron-phonon scattering rates on the application of the mechanical BC within the dielectric continuum approach. We study systems with widely varying geometries including planar quantum wells, cylindrical quantum wires, and spherical quantum dots. We calculate the scalar potentials of the confined phonons and the corresponding phonon structure factors which enter the scattering rates. Calculations are made both with and without the additional constraint given by the mechanical BC.⁷ It is found that although the individual phonons for the two models differ substantially, the results for the total scattering rates for each set of confined phonons are *identical*. We ascribe this interesting behavior to the fact that measurable quantities arising from the confined phonons involve sums over complete sets of degenerate phonon states. We also find that the sums for the scattering rates converge

more rapidly if the phonons do not satisfy the mechanical BC.

II. DIELECTRIC CONTINUUM APPROACH

The dielectric continuum approach¹ is described briefly now. We consider a system consisting of one polar semiconductor with dielectric function $\epsilon_1(\omega)$ embedded in another with dielectric function $\epsilon_2(\omega)$. Each dielectric function is frequency dependent and is assumed to be isotropic and independent of wave vector \mathbf{k} . Each material is taken to be characterized by dispersionless LO and TO modes, and the dielectric functions are taken to be

$$\epsilon_i(\omega) = \epsilon_\infty \frac{\omega_{\text{LO},i}^2 - \omega^2}{\omega_{\text{TO},i}^2 - \omega^2}, \quad (1)$$

with i corresponding to the material either inside or outside of the nanostructure. No net charge resides in either material, so within each the quantity $\nabla \cdot \mathbf{D} = \nabla \cdot [\epsilon_i(\omega) \mathbf{E}] = \epsilon_i(\omega) \nabla \cdot \mathbf{E}$ vanishes where \mathbf{D} is the displacement field, and \mathbf{E} is the electric field. This gives $\epsilon_i(\omega) \nabla \cdot \mathbf{E} = 0$ in each material.

Interface modes satisfy the condition $\nabla \cdot \mathbf{E} = 0$ in each material and the electromagnetic BC's that \mathbf{E}_\parallel and $D_\perp = \epsilon E_\perp$ are continuous across the interface. Here we are interested in the confined phonon modes, whose spatial dependence satisfies electromagnetic BC's and whose frequency satisfies the equation $\epsilon_i(\omega) = 0$. These conditions describe phonons confined in material i with frequency $\omega_{\text{LO},i}$. The ionic displacements \mathbf{u} are proportional to $\mathbf{E} = -\nabla \Psi$, where Ψ is the scalar potential.⁸ Because \mathbf{E} vanishes in the other material and \mathbf{E}_\parallel is continuous, Ψ is constant on the interface. By a simple gauge transformation this is equivalent to Ψ vanishing there. The ionic displacements \mathbf{u}^{conf} of the confined phonons are orthogonal to the displacements $\mathbf{u}^{\text{if}}[\propto \mathbf{E}^{\text{if}}(\mathbf{r})]$ of the interface phonons in the sense that $\int d^3r \mathbf{u}^{\text{conf}}(\mathbf{r}) \cdot [\mathbf{u}^{\text{if}}(\mathbf{r})]^* = 0$. This orthogonality relation is derived straightforwardly by using Green's first identity, the fact that Ψ^{conf} vanishes at the boundary, and the fact that $\nabla \cdot \mathbf{E}^{\text{if}}$ vanishes away from the boundary.

Hence any scalar function which vanishes at the interface can be used to represent a confined mode. The Hilbert space of such functions is of infinite dimension, and because the confined phonons are degenerate, any orthonormal set of modes which spans the space forms an adequate basis. The choice of particular modes to form such a basis is arbitrary, but two specific choices have

been discussed recently. Here we will call these model *A* and model *B*. Historically the confined phonon potentials in the dielectric continuum approach for quantum wells have usually been chosen to be simple sine and cosine functions, for circular wires chosen to be Bessel functions, and for spherical dots to be spherical Bessel functions. This is equivalent to their being chosen to be eigenfunctions of the Laplacian operator ∇^2 . We will take model *A* to be given by this choice. Thus model *A* is just the usual dielectric continuum model.¹ These potentials however do not satisfy the mechanical BC because the normal component of the ionic displacements does not vanish at the interface. For model *B* the potentials are chosen in such a way that they satisfy the mechanical BC as well as the electromagnetic BC. Thus model *B* is similar to that considered by Huang and Zhu^{4,9} but here fully orthogonalized. In the next section we calculate these phonons for three different geometries: well, wire, and dot.

III. PHONONS

In this section we compare confined phonons which satisfy only the electromagnetic BC (model *A*) with phonons satisfying both the electromagnetic and the mechanical BC's (model *B*). We make this comparison for three different geometries: quantum wells, cylindrical quantum wires, and spherical quantum dots. From symmetry considerations for these systems the scalar potentials for the confined LO phonons¹⁰ can be written in the form $\Psi(\mathbf{r}) = S_\nu(\xi, \eta) \psi_\nu(\chi)$, where (ξ, η, χ) form an orthogonal coordinate system, ν is a symmetry-related quantum number, $S_\nu(\xi, \eta)$ is a simple function, and $\psi_\nu(\chi)$ is the "reduced" potential. $\chi = a$ defines the interface of the nanostructure, whose size thus equals $2a$. Examples are listed in the first five columns of Table I.

First we consider confined modes which satisfy the electromagnetic BC and which are eigenfunctions of ∇^2 (model *A*). We represent these reduced potentials as $\psi_{\nu n}^{(A)}(\chi) = f_\nu(Q_{\nu n}^{(A)} \chi)$, where the quantum number n is unrelated to the mode's symmetry. (Usually n is taken to be the number of nodes in ψ —the so-called confinement number.) Examples are shown in Table I. The wave vector $Q_{\nu n}^{(A)}$ satisfies the electromagnetic BC that $f_\nu(Q_{\nu n}^{(A)} a) = 0$. This BC yields an infinite, discrete set of $Q_{\nu n}^{(A)}$ for each ν . The specific values of $Q_{\nu n}^{(A)}$ are important for high-resolution spectroscopies such as Raman scattering which can discern the differences in energy between phonons having different confinement numbers. Some

TABLE I. Parameters giving the coordinates (ξ, η, χ) , quantum numbers (ν) , and wave functions $(S_\nu, f_\nu, g_\nu, h_\nu)$ for the confined optical phonons described in the text. The functions $P_l^m(X)$, $J_m(X)$, $j_l(X)$, $I_m(X)$, and $K_m(X)$ are associated Legendre polynomials, Bessel functions, spherical Bessel functions, modified Bessel functions, and modified Hankel functions, respectively.

Nanostructure	(ξ, η)	χ	ν	$S_\nu(\xi, \eta)$	$f_\nu(X)$	$g_\nu(\chi)$	$h_\nu(\chi)$
Well, symmetric	(x, y)	z	\bar{k}	$\exp i\bar{k} \cdot (\hat{\mathbf{i}}x + \hat{\mathbf{j}}y)$	$\cos X$	$\cosh kz$	$\exp -k z $
Well, antisymmetric	(x, y)	z	\bar{k}	$\exp i\bar{k} \cdot (\hat{\mathbf{i}}x + \hat{\mathbf{j}}y)$	$\sin X$	$\sinh kz$	$\frac{ z }{z} \exp -k z $
Wire	(z, ϕ)	r	k, m	$\exp i(kz - m\phi)$	$J_m(X)$	$I_m(kr)$	$K_m(kr)$
Dot	(θ, ϕ)	r	l, m	$P_l^m(\cos \theta) \exp im\phi$	$j_l(X)$	r^l	r^{-l-1}

examples of the reduced potentials $\psi_{\nu n}^{(A)}(\chi)$ are shown in Fig. 1 for LO phonons confined to quantum wells, quantum wires, and quantum dots. For $(\nu, n) \neq (\nu', n')$ it is straightforward to verify that the ionic displacement $\mathbf{u}_{\nu n}^{(A)}[\propto \nabla \Psi_{\nu n}^{(A)}(\mathbf{r})]$ is orthogonal to $\mathbf{u}_{\nu' n'}^{(A)}$. The transverse displacement $\mathbf{u}_{\parallel}^{(A)}$ vanishes at the interface (and thus is continuous), but the normal displacement $u_{\perp}^{(A)}$ does not.

Next we consider confined modes which satisfy both the electromagnetic and the mechanical BC's (model *B*). Such modes have been used to model macroscopically the results of lattice dynamics calculations by Huang and Zhu for a superlattice⁴ and by Zhu for an array of quantum wires.⁹ One shortcoming of the Huang-Zhu modes is that they are orthogonal only for $k \ll a^{-1}$, where $2a$ is the well width, and k is the component of the phonon wave vector along the well. However, values of $k = O(a^{-1})$ give important contributions to electron-phonon scattering processes for most nanostructure sizes. This characteristic of the Huang-Zhu modes can be remedied by Gram-Schmidt orthogonalization.⁶ However, a more systematic method has been given for a superlattice by Chen.¹¹ This technique yields confined phonons which satisfy both the electromagnetic and the mechanical BC's, and which are mutually orthogonal at all values of k . The results of Ref. 11 can be extended to other nanostructures such as a cylindrical quantum wire or a spherical dot, and we do so here.

Satisfaction of both the electromagnetic and the mechanical BC's is attained by choosing a different form for the reduced potential, represented as $\psi_{\nu n}^{(B)}(\chi)$ where $\Psi^{(B)}(\mathbf{r}) = S_{\nu}(\xi, \eta)\psi_{\nu n}^{(B)}(\chi)$. By setting $\psi_{\nu n}^{(B)}(\chi) = g_{\nu}(a)f_{\nu}(Q_{\nu n}^{(B)}\chi) - g_{\nu}(\chi)f_{\nu}(Q_{\nu n}^{(B)}a)$ the electromagnetic BC is automatically satisfied. The function $g_{\nu}(\chi)$ is regular at the origin, diverges at infinity, and is chosen so that $S_{\nu}(\xi, \eta)g_{\nu}(\chi)$ has vanishing Laplacian. Specific forms for $g_{\nu}(\chi)$ are given in Table I. The wave number $Q_{\nu n}^{(B)}$ satisfies the transcendental equation

$$Q_{\nu n}^{(B)} g_{\nu}(a) f'_{\nu}(Q_{\nu n}^{(B)} a) = g'_{\nu}(a) f_{\nu}(Q_{\nu n}^{(B)} a). \quad (2)$$

From this form for Eq. (2) and $\psi_{\nu n}^{(B)}(\chi)$ it is evident that $\Psi^{(B)}(\mathbf{r})$ also satisfies the mechanical BC. Equation (2) yields an infinite, discrete set of $Q_{\nu n}^{(B)}$ for each ν . For $(\nu, n) \neq (\nu', n')$ it is again straightforward to verify that the phonon displacements are orthogonal. Note that the

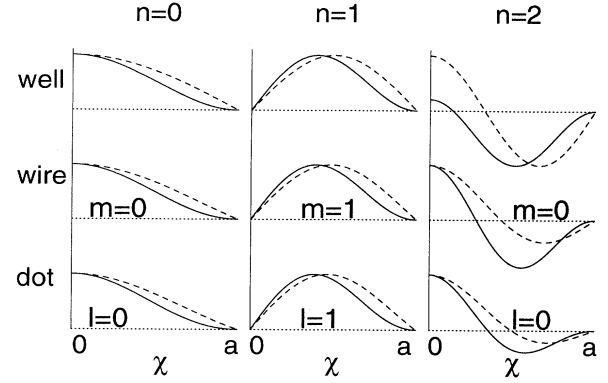


FIG. 1. Reduced potentials of confined phonons which obey the electromagnetic BC. The solid (dashed) lines indicates modes which do (not) also satisfy the mechanical BC. For the well and the wire the dimensionless wave number ka is chosen to equal unity. For even (odd) confinement number n the potential is symmetric (antisymmetric) with respect to reflection through the middle of the nanostructure, represented by the vertical solid lines.

confined phonons in both models *A* and *B* are orthogonal to the interface modes. Some examples of $\psi_{\nu n}^{(B)}(\chi)$ for quantum wells, quantum wires, and quantum dots are shown in Fig. 1, where they are compared to $\psi_{\nu n}^{(A)}(\chi)$. There it is seen that the main qualitative difference between the potentials of the confined phonons for models *A* and *B* involves their appearance near the interface, where those of model *A* go to zero linearly but those of model *B* go to zero quadratically. Hence the enforcement of the mechanical BC alters the appearance of individual phonons. On the other hand, physically observable quantities, such as electron-phonon scattering rates or mean-squared displacements, involve sums over all of the phonons. We investigate this topic in the next section.

IV. ELECTRON-PHONON SCATTERING RATES

As an example of a physically measurable quantity we consider the scattering rate due to the Fröhlich interaction between the optical phonon modes and electrons. The scattering rate of an electron from an initial state α to a final state β accompanied by the emission or absorption of a phonon is given by

$$\Gamma_{\alpha \rightarrow \beta} = \frac{2\pi e^2}{\hbar} \sum_{\mu} C_{\mu} [N(\omega_{\mu}) + \frac{1}{2} \pm \frac{1}{2}] \left| \int d^3 r \Pi_{\alpha}(\mathbf{r}) \Pi_{\beta}^*(\mathbf{r}) \Psi_{\mu}(\mathbf{r}) \right|^2 \delta(E_{\beta} - E_{\alpha} \pm \hbar \omega_{\mu}). \quad (3)$$

Here $\Pi_{\alpha}(\mathbf{r})$ are the electron wave functions, E_{α} are the electron energies, $\Psi_{\mu}(\mathbf{r})$ are the scalar potentials associated with the phonons, C_{μ} are the normalizations for these phonons, and $N(\omega) = [\exp \frac{\hbar \omega}{k_B T} - 1]^{-1}$. The sum over μ includes both interface phonons and confined phonons, and the top (bottom) sign is taken for phonon emission (absorption). Here we consider the contribution of the confined phonons to the sum in Eq. (3). The confined phonons are taken to be dispersionless, and their normalizations C_{μ} are easy to compute. The confined mode contribution to the scattering rate can be written in the form

$$\Gamma_{\alpha \rightarrow \beta}^{\text{conf}} = \frac{e^2 [N(\omega_{\text{LO}}) + \frac{1}{2} \pm \frac{1}{2}] \delta(E_{\beta} - E_{\alpha} \pm \hbar \omega_{\text{LO}})}{\omega_{\text{LO}}} \left\{ \frac{9\epsilon_{\infty}(\omega_{\text{LO}}^2 - \omega_{\text{TO}}^2)}{V(\epsilon_{\infty} + 2)^2} \right\} \iint d^3 r d^3 r' \Pi_{\alpha}(\mathbf{r}) \Pi_{\beta}^*(\mathbf{r}) \Pi_{\alpha}^*(\mathbf{r}') \Pi_{\beta}(\mathbf{r}') \rho^{\text{conf}}(\mathbf{r}, \mathbf{r}'), \quad (4)$$

where V is the nanostructure volume. The “structure factor” corresponding to the confined phonons is given by

$$\rho^{\text{conf}}(\mathbf{r}, \mathbf{r}') = V \sum_i \frac{\Psi_i(\mathbf{r})\Psi_i^*(\mathbf{r}')}{\int d^3r'' |\nabla\Psi_i(\mathbf{r}'')|^2} \quad (5)$$

in which the sum over i includes only confined phonons. A similar form for the scattering rate has been given in Ref. 3. The normalization of the confined phonon displacements \mathbf{u} is given by the factor in curly brackets in Eq. (4) and the denominator in Eq. (5). Physically interesting quantities such as scattering rates depend not on the individual phonon potentials but rather on the combination which appears in Eq. (5).

For the symmetric nanostructures discussed here $\rho(\mathbf{r}, \mathbf{r}')$ is a sum of contributions from several symmetry classes, given by ν in Table I. For example, for a quantum well at a given k there are contributions that are even or odd with respect to reflections through the well’s mirror plane. In this case it becomes convenient to discuss a symmetry decomposition of the structure factor given by $\rho(\mathbf{r}, \mathbf{r}') = \sum_\nu S_\nu(\xi, \eta) S_\nu^*(\xi', \eta') \rho_\nu(\chi, \chi')$. The reduced structure factor ρ_ν^{conf} is given by

$$\rho_\nu^{\text{conf}}(\chi, \chi') = V \sum_n \frac{\psi_{\nu n}(\chi)\psi_{\nu n}^*(\chi')}{\int d^3r'' |\nabla\Psi_{\nu n}(\mathbf{r}'')|^2}. \quad (6)$$

This quantity involves a sum over the infinite set of confinement numbers n .

The contributions of the confined modes to the reduced structure factor for the symmetric modes of a quantum well are shown in Figs. 2(a) and 2(b), and those for the antisymmetric modes in Figs. 2(c) and 2(d). Results for confined phonons satisfying only the electromagnetic BC (model *A*) are shown in panels (a) and (c), and those for phonons satisfying both the electromagnetic and the mechanical BC’s (model *B*) are shown in panels (b) and (d). The most important thing to note is that the results for the fully summed structure factors are *independent* of whether the phonons appearing in the sum satisfy the mechanical BC in addition to the electromagnetic BC. We have also performed these calculations for a cylindrical wire and a spherical dot, and we again find that the structure factors are independent of mechanical BC. This interesting result is expected to hold for all nanostructure geometries, not only the simple ones considered here.

A second feature of interest is the rate at which the structure factor converges as a function of the maximum confinement number n_{max} retained in the sum. For small to moderate values of the symmetry index ν (e.g., k , m , etc.) the sum is fairly well converged when $n_{\text{max}} > 5$, but for large ν the cusp at $\chi = \chi'$ seen in Fig. 2 becomes very sharp, which causes the sum to converge quite slowly. The sum for ρ^{conf} converges more rapidly in model *A* than in model *B*. This is because the individual contributions in model *A*, like ρ^{conf} itself, approach zero linearly as χ approaches a , whereas in model *B* the individual contributions approach zero quadratically in this region. Hence even though model *B* phonons compare more favorably with lattice dynamics results, model *A* phonons

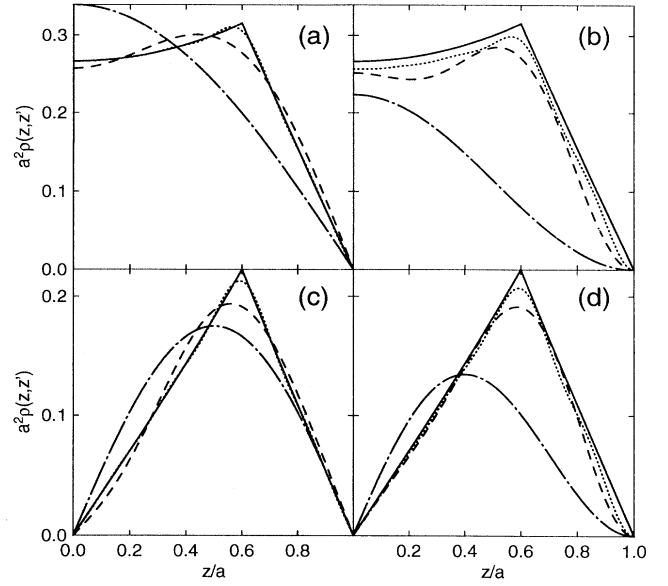


FIG. 2. Reduced structure factors from Eq. (6) for the optical phonons confined to the interior of a quantum well. The reduced structure factors are evaluated for $k = 1.0/a$ and $z' = 0.6a$. For panels (a) and (b) the phonon potentials are symmetric with respect to reflection, and for (c) and (d) they are antisymmetric. For panels (b) and (d) the phonons satisfy the mechanical BC at the interfaces, and for (a) and (c) they do not. The dot-dashed, dashed, dotted, and solid lines indicate a truncation of the sum in Eq. (6) after $n_{\text{max}} = 1, 3, 10$, and ∞ terms, respectively.

converge more quickly in calculations of such observable quantities as electron-phonon scattering rates.

V. RELATION BETWEEN CONFINED PHONONS AND INTERFACE PHONONS

In order to understand the equality of the structure factors calculated using different sets of confined phonons it is useful to derive a more elegant formula for $\rho^{\text{conf}}(\mathbf{r}, \mathbf{r}')$, starting from Eq. (5). The functions $\Psi_j(\mathbf{r})$ form a complete set of scalar functions vanishing at the interface. Their displacements are orthogonal which gives $\delta_{ij} \propto \int d^3r \nabla\Psi_i \cdot \nabla\Psi_j^* = - \int d^3r \Psi_i \nabla^2\Psi_j^*$ from Green’s first identity. Multiplying both sides of Eq. (5) by $\nabla'^2\Psi_j(\mathbf{r}')$, integrating over \mathbf{r}' , and using Green’s theorem yields

$$\Psi_j(\mathbf{r}) = - \int d^3r' \Psi_j(\mathbf{r}') \nabla'^2 \rho^{\text{conf}}(\mathbf{r}, \mathbf{r}'). \quad (7)$$

Equation (7) is true for all j , which implies that $\rho^{\text{conf}}(\mathbf{r}, \mathbf{r}') = V\Theta(\mathbf{r})\Theta(\mathbf{r}')[\frac{1}{4\pi|\mathbf{r}-\mathbf{r}'|} + \Lambda(\mathbf{r}, \mathbf{r}')]$, where $\Lambda(\mathbf{r}, \mathbf{r}')$ is a function which has vanishing Laplacian and which causes $\rho^{\text{conf}}(\mathbf{r}, \mathbf{r}')$ to vanish at the boundaries. The function $\Theta(\mathbf{r})$ is defined to vanish outside the nanostructure and to equal unity inside it and on the boundaries.¹² We show in the Appendix that the unique solution for these conditions is¹³

$$\rho^{\text{conf}}(\mathbf{r}, \mathbf{r}') = V\Theta(\mathbf{r})\Theta(\mathbf{r}') \times \left[\frac{1}{4\pi|\mathbf{r} - \mathbf{r}'|} - \sum_{\lambda} \frac{\Phi_{\lambda}(\mathbf{r})\Phi_{\lambda}^*(\mathbf{r}')}{\int d^3r'' |\nabla\Phi_{\lambda}(\mathbf{r}'')|^2} \right]. \quad (8)$$

The function $\Phi_{\lambda}(\mathbf{r})$ is the scalar potential generated by the λ th *interface* phonon (calculated in the nonretarded limit) of the nanostructure¹⁴ and so has vanishing Laplacian everywhere except at the interfaces.¹ For nanostructures of general shape these phonons are obtained straightforwardly by an integral equation method,¹⁵ and for a nanostructure with high symmetry such as a slab,

cylinder, or sphere there exists exactly one interface phonon for each ν . The interface phonon potential is given simply by

$$\Phi_{\nu} = S_{\nu}(\xi, \eta) \times \begin{cases} g_{\nu}(\chi)h_{\nu}(a), & \chi \leq a \\ g_{\nu}(a)h_{\nu}(\chi), & \chi \geq a, \end{cases} \quad (9)$$

where $h_{\nu}(\chi)$ is chosen so that $S_{\nu}(\xi, \eta)h_{\nu}(\chi)$ has vanishing Laplacian and so that $h_{\nu}(\chi)$ vanishes at infinity.¹⁶ Specific forms for $h_{\nu}(\chi)$ are given in Table I. The reduced structure factor is then given by

$$\rho_{\nu}^{\text{conf}}(\chi, \chi') = \frac{V\Theta(\chi)\Theta(\chi')h_{\nu}(a)g_{\nu}(\chi_{<})[g_{\nu}(a)h_{\nu}(\chi_{>}) - g_{\nu}(\chi_{>})h_{\nu}(a)]}{\int d^3r'' |\nabla\Phi_{\nu}(\mathbf{r}'')|^2}, \quad (10)$$

where $\chi_{>}[\chi_{<}] = \max(\chi, \chi')[\min(\chi, \chi')]$. Equations (8) and (10) form an elegant link between the contributions of the confined phonons and those of the interface phonons. The structure factors obtained from Eq. (10) are given by the solid lines in Fig. 2. Note that in Eqs. (8) and (10) the structure factors can be calculated using only the interface modes for the nanostructure. The results obtained in this way are indistinguishable from those obtained by direct summation of an infinite number of the confined phonons, which are also given by the solid lines in Fig. 2. The cusp at $\chi = \chi'$ seen in Fig. 2 derives from the singularity at $\mathbf{r} = \mathbf{r}'$ in the first term of Eq. (8).

Equations (8) and (10) have several advantages over Eqs. (5) and (6). For the highly symmetric nanostructures such as those considered here the direct summation on the right-hand side of Eq. (6) contains an infinite number of terms which converge slowly (especially for large ν), whereas the right-hand side of Eq. (10) has only two terms. The first term on the right-hand side of Eq. (10) derives from the singular term in Eq. (8) and the second term from the interface phonon of that particular symmetry. Also, for most nanostructure shapes having lower symmetry than those considered here it is possible to generate the interface modes reasonably straightforwardly¹⁵ but much more difficult to denumerate a complete set of confined modes. Two examples of this are the confined phonons of a wire having an oval cross section¹⁷ or the optical phonons confined in the region outside of a wire having a rectangular cross section.¹⁸ In these cases the only reasonable option is to use Eq. (8).

VI. SUMMARY

In the present work we have studied the effect of the mechanical BC on the confined LO phonons in nanostructures of different shapes. We find that the use of this BC in addition to the electromagnetic BC alters the scalar potentials for individual phonons but has no effect upon physical observables such as electron-phonon scattering rates in the absence of bulk phonon dispersion. We note that in previous work^{2,3,5} small, nonzero differences were found between the results for scatter-

ing rates calculated using the usual dielectric continuum model (model A) phonons and the phonons of Huang and Zhu.^{4,9} We ascribe these differences to the fact that the Huang-Zhu modes are not orthogonal. More recently Haupt and Wendler⁶ used the Gram-Schmidt technique to orthogonalize the Huang-Zhu phonons, but they still found that the resulting scattering rates to be smaller than those for the dielectric continuum model phonons. We ascribe this discrepancy to the small number of modes ($n_{\text{max}} = 3$ for each symmetry) included in their calculations. From Fig. 2 in the present work it is seen that the structure factor is not well converged for such a small number of modes and that significant underestimation of the scattering rate is expected for phonons satisfying the mechanical BC.

In demonstrating the independence of physical observables upon the mechanical BC we have generated a formula [Eq. (8)] for the structure factor of LO phonons confined to nanostructures of arbitrary shape. This formula is interesting in that it relates the contribution from the confined phonons to that from the interface phonons. This feature proves useful when one deals with low symmetry geometries of experimental interest or when Eq. (5) converges slowly. The only requirement needed to obtain Eq. (8) is that the confined phonon modes form a complete set and satisfy the electromagnetic BC. Thus we argue that any complete orthonormal set of confined modes which satisfy the electromagnetic BC will give the same result for an observable such as the electron-phonon scattering rate, a quantity which necessarily involves a sum over all phonons. We also note that this structure factor represents the confined-phonon contribution to a variety of phenomena which involve electron-phonon interactions in first order perturbation theory. Indeed it can be argued that essentially all physical observables involving electron-phonon interactions that can be treated in perturbation theory are described by this function. Such quantities include phonon induced electronic relaxation rates, electron-phonon scattering rates, and mean squared displacements. The contributions of the confined phonons to all of these quantities will be independent of the mechanical BC in the absence of dispersion in the optical phonons.

Another interesting example involves the Raman scat-

tering cross section, which has been of considerable interest in quantum well systems.¹⁹ In a model which has no bulk optical phonon dispersion the Raman intensity is independent of the mechanical BC. However such experiments can resolve the small energy differences between the confined modes, and a description which includes the small LO phonon dispersion is needed. Then the total Raman cross section is only weakly dependent on the application of the mechanical BC even though the scattering by individual confined phonons may be sensitive to it.

ACKNOWLEDGMENTS

This work was supported in part by contracts from the U. S. Office of Naval Research (P.A.K. and T.L.R.).

APPENDIX A: STRUCTURE FACTOR

The scalar potentials $\Phi_\lambda(\mathbf{r})$ generated by the interface phonons of the nanostructure form a complete set of functions having vanishing Laplacian. By using this fact, Eq. (5), and Eq. (7), we obtain the result that the structure factor can be written in the form

$$\rho^{\text{conf}}(\mathbf{r}, \mathbf{r}') = V\Theta(\mathbf{r})\Theta(\mathbf{r}') \times \left[\frac{1}{4\pi|\mathbf{r} - \mathbf{r}'|} - \sum_{\lambda\lambda'} M_{\lambda\lambda'} \Phi_\lambda(\mathbf{r})\Phi_{\lambda'}^*(\mathbf{r}') \right], \quad (\text{A1})$$

where M is a Hermitian matrix to be determined. We determine M by evaluating Eq. (A1) at a point $\mathbf{r}' \equiv \mathbf{r}_b$ on the boundary to yield

$$\frac{1}{4\pi|\mathbf{r} - \mathbf{r}_b|} = \sum_{\lambda\lambda'} M_{\lambda\lambda'} \Phi_\lambda(\mathbf{r})\Phi_{\lambda'}^*(\mathbf{r}_b). \quad (\text{A2})$$

Operating on both sides of Eq. (A2) with $\int d^3r [\nabla\Phi_{\lambda''}^*(\mathbf{r}) \cdot \nabla]$ yields

$$\int d^3r \nabla\Phi_{\lambda''}^*(\mathbf{r}) \cdot \nabla \left[\frac{1}{4\pi|\mathbf{r} - \mathbf{r}_b|} \right] = \sum_{\lambda\lambda'} M_{\lambda\lambda'} \Phi^*(\mathbf{r}_b) \left[\int d^3r \nabla\Phi_{\lambda''}^*(\mathbf{r}) \cdot \nabla\Phi_\lambda(\mathbf{r}) \right]. \quad (\text{A3})$$

In Ref. 15 it is shown that the bracketed quantity on the right-hand side of Eq. (A3) vanishes if $\lambda \neq \lambda''$, a fact related to the orthogonality of the interface phonons. Using this fact and Green's first identity yields

$$\frac{\Phi_\lambda^*(\mathbf{r}_b)}{\int d^3r |\nabla\Phi_\lambda(\mathbf{r})|^2} = \sum_{\lambda'} M_{\lambda\lambda'} \Phi_{\lambda'}^*(\mathbf{r}_b). \quad (\text{A4})$$

Because Eq. (A4) is true for all boundary points \mathbf{r}_b , it follows that $M_{\lambda\lambda'} = \delta_{\lambda\lambda'}/\int d^3r |\nabla\Phi_\lambda(\mathbf{r})|^2$ and that the structure factor is given by Eq. (8).

¹See, e.g., M. V. Klein, IEEE J. Quantum Electron. **QE-22**, 1760 (1986).

²H. Rucker, E. Molinari, and P. Lugli, Phys. Rev. B **44**, 3463 (1991).

³H. Rucker, E. Molinari, and P. Lugli, Phys. Rev. B **45**, 6747 (1992).

⁴Kun Huang and Bangfen Zhu, Phys. Rev. B **38**, 13377 (1988).

⁵S. Rudin and T. L. Reinecke, Phys. Rev. B **41**, 7713 (1990); **43**, 9298(E) (1991).

⁶R. Haupt and L. Wendler, Phys. Rev. B **44**, 1850 (1991).

⁷Continuum approaches which satisfy certain components of the mechanical, but not the electromagnetic, BC, also have been introduced [e.g., B. K. Ridley, Phys. Rev. B **39**, 5282 (1989)]. It has been pointed out (Refs. 2 and 3) that the resulting confined phonons ("guided" phonons) do not agree well with lattice dynamics calculations. Thus we do not study such approaches here.

⁸The vector potential \mathbf{A} of these modes is zero because LO phonons do not couple with transverse electromagnetic fields.

⁹Bang-fen Zhu, Phys. Rev. B **44**, 1926 (1991).

¹⁰Here we consider confined LO phonons, which have vanishing displacement field ($\mathbf{D} = \epsilon\mathbf{E}$) but nonvanishing electric

field ($\mathbf{E} = -\nabla\Phi$). With minor changes much of the formalism presented here also applies to confined TO phonons, which have nonvanishing \mathbf{D} but vanishing \mathbf{E} and Φ and so interact only weakly with electrons.

¹¹C. D. Chen, Solid State Commun. **81**, 785 (1992). In this reference it is seen that the confined phonons agree better with lattice dynamics results than do those of Ref. 4.

¹²For the "excluded" modes (i.e., phonons confined *outside* the nanostructure) the structure factor $\rho^{\text{excl}}(\mathbf{r}, \mathbf{r}')$ is obtained by using $1 - \Theta$ instead of Θ in this and subsequent formulas.

¹³The integrand appearing in this and subsequent equations is nonzero both inside and outside of the nanostructure. The volume of integration includes both regions.

¹⁴It might be noted that to each λ there correspond two different interface modes having identical (except for overall normalization) scalar potentials $\Phi_\lambda(\mathbf{r})$ (Ref. 15).

¹⁵P. A. Knipp and T. L. Reinecke, Phys. Rev. B **46**, 10310 (1992).

¹⁶R. Englman and R. Ruppin, J. Phys. C **1**, 614 (1968).

¹⁷P. Knipp and T. L. Reinecke, Phys. Rev. B **45**, 9091 (1992).

¹⁸P. Knipp and T. L. Reinecke, Phys. Rev. B **48**, 5700 (1993).

¹⁹Kun Huang, Bang-fen Zhu, and Hui Tang, Phys. Rev. B **41**, 5825 (1990).